This article was published in Biochemical and biophysical research communications. 2020 Aug 27;529(3):793-798
doi: 10.1016/j.bbrc.2020.06.045.



# Genetic knockout and pharmacologic inhibition of NCX1 attenuate hypoxia-induced pulmonary arterial hypertension

Asahi Nagata[a,b,1], Hideaki Tagashira[a,1], Satomi Kita[a,c,*], Tomo Kita[a], Naoko Nakajima[a], Kohtaro Abe[d], Akinori Iwasaki[b], Takahiro Iwamoto[a,*]

[a]*Department of Pharmacology, Faculty of Medicine, Fukuoka University, Fukuoka, Japan*

[b]*Department of General Thoracic, Breast and Pediatric Surgery, Faculty of Medicine, Fukuoka University, Fukuoka, Japan*

[c]*Department of Pharmacology, Faculty of Pharmaceutical Sciences, Tokushima Bunri University, Tokushima, Japan*

[d]*Department of Cardiovascular Medicine, Kyushu University Graduate School of Medical Sciences, Fukuoka, Japan*

**Footnote**

* Corresponding authors at: Department of Pharmacology, Faculty of Medicine, Fukuoka University, 7-45-1 Nanakuma, Jonan-ku, Fukuoka 814-0180, Japan. Fax: +81 92 865 4384.

E-mail addresses: tiwamoto@fukuoka-u.ac.jp (T. Iwamoto), satokita@fukuoka-u.ac.jp (S. Kita).

[1] These two authors contributed equally.

**Abstract**

The $Na^+/Ca^{2+}$ exchanger type-1 (NCX1) is a bidirectional transporter that is controlled by membrane potential and transmembrane gradients of $Na^+$ and $Ca^{2+}$. Vascular smooth muscle NCX1 plays an important role in intracellular $Ca^{2+}$ homeostasis and $Ca^{2+}$ signaling. We found that NCX1 was upregulated in the pulmonary arteries of mice exposed to chronic hypoxia (10% $O_2$ for 4 weeks). Hence, we investigated the pathophysiological role of NCX1 in hypoxia-induced pulmonary arterial hypertension (PAH), using NCX1-heterozygous ($NCX1^{+/-}$) mice, in which NCX1 expression is reduced by half, and SEA0400, a specific NCX1 inhibitor. $NCX1^{+/-}$ mice exhibited attenuation of hypoxia-induced PAH and right ventricular (RV) hypertrophy compared with wild-type mice. Furthermore, continuous administration of SEA0400 (0.5 mg/kg/day for 4 weeks) by osmotic pumps significantly suppressed hypoxia-induced PAH and pulmonary vessel muscularization, with a slight reduction in RV hypertrophy. These findings indicate that the upregulation of NCX1 contributes to the development of hypoxia-induced PAH, suggesting that NCX1 inhibition might be a novel approach for the treatment of PAH.

**Keywords:** Pulmonary arterial hypertension, Vascular remodeling, Hypoxia, Genetic knockout, NCX1 inhibitor

## 1. Introduction

Pulmonary arterial hypertension (PAH) is a progressive and intractable disease characterized by increased pulmonary arterial tone and vascular remodeling, eventually resulting in right heart failure [1,2]. Histologically, patients with severe PAH exhibit small pulmonary arterial wall thickening, occlusive neointima, and formation of plexiform lesions originating from remodeled pulmonary arteries [3]. Such pulmonary arteriopathy can be triggered by a wide spectrum of genetic and environmental stimuli, including chronic hypoxia and inflammation [4,5]. Chronic hypoxia-induced PAH is clinically caused by chronic obstructive pulmonary disease (COPD) and obstructive sleep apnea. Actually, in experimental animals, prolonged exposure to hypoxia generates the most commonly used PAH models [5,6]. Currently, several vasodilating drugs are used for preventing the progression of PAH, but their therapeutic effects are still insufficient [1]. Therefore, there is an urgent need for finding novel therapeutic targets of PAH.

Increased intracellular $Ca^{2+}$ concentration in pulmonary arteries is a critical trigger for pulmonary arterial hypercontraction and vascular remodeling [7], leading to the initiation and progression of PAH. Previous studies have shown that chronic hypoxia causes abnormally enhanced $Ca^{2+}$ signaling in pulmonary arteries, although the underlying molecular mechanisms are still controversial [5,7].

The $Na^{+}/Ca^{2+}$ exchanger type-1 (NCX1) is a bidirectional $Ca^{2+}$ transporter controlled by membrane potential and transmembrane gradients of $Na^{+}$ and $Ca^{2+}$, which plays an important role in intracellular $Ca^{2+}$ homeostasis and $Ca^{2+}$ signaling [8,9]. NCX1 is ubiquitously

expressed in several tissues, and is especially abundant in heart and blood vessels. Previous studies utilizing genetically altered mice and selective inhibitors for NCX1 revealed that NCX1 is pathophysiologically involved in the development of ischemic diseases of various organs [10-12] and salt-sensitive hypertension [13]. In this study, we found that NCX1 is excessively expressed in the pulmonary arteries of hypoxia-induced PAH model mice. However, the role of NCX1 in the pathogenesis of hypoxia-induced PAH is clearly unknown. Our studies with NCX1-heterozygous mice and specific NCX1 inhibitor provide compelling evidence that upregulation of NCX1 contributes to the development of hypoxia-induced PAH.

## 2. Materials and methods

### *2.1. Animals*

NCX1-heterozygous ($NCX1^{+/-}$) mice were generated as reported previously [14,15]. C57BL/6J mice were purchased from Japan SLC (Japan). All mice used were males and they were housed under diurnal lighting conditions (light period 8:00 a.m. to 8:00 p.m.) and allowed access to normal raw chow and plain drinking water *ad libitum*. The experimental designs and all procedures were conducted in accordance with the Animal Care Guidelines of the Animal Experimental Committees of Fukuoka University.

### *2.2. Drugs*

SEA0400 (2-[4-[(2,5-difluorophenyl)methoxy]phenoxy]-5-ethoxyaniline) were synthesized by procedures described previously [15], and were finally identified with $^{1}$H NMR

spectra and Mass spectra. Other chemical agents were of the highest grade available from Sigma-Aldrich (USA) or Fujifilm Wako Chemicals (Japan).

*2.3. Hypoxia-induced PAH model experiments*

Eight- to 10-week-old mice were placed in an acrylic chamber exposed to normobaric hypoxia (10% $O_2$) or normoxia (21% $O_2$) for 4 weeks. Hypoxic gas (10% $O_2$) was generated by absorption-type oxygen concentrator to utilized exhaust air (Teijin, Japan) and continuously monitored by a digital oxygen monitor (Ichinen Jikco, Japan).

To measure right ventricular hemodynamics, mice were anesthetized intraperitoneally with mixture of medetomidine (0.3 mg/kg), midazolam (4 mg/kg), and butorphanol (5 mg/kg). Right ventricular systolic pressure (RVSP) was measured by a 1.4F mouse pressure catheter (Millar, USA) advanced into the right ventricle (RV) through the right jugular vein, and recorded using a LabChart 8 software (AD Instruments, USA). To evaluate the extent of RV hypertrophy, hearts were then isolated after exsanguination. The RV was dissected from the left ventricle and septum (LV+S), and the weight ratio of RV/(LV+S) was determined.

*2.4. Immunohistochemistry*

Lungs were perfused with phosphate-buffered saline, followed by fixation in 4% paraformaldehyde. Fixed left lungs were embedded in paraffin and subsequently sectioned at a thickness of 5 μm. For immunohistochemical staining, de-paraffinization and antigen retrieval were performed using Histofine regents (Nichirei Bio, Japan) under the manufacturer's

protocol. The sections were blocked with 3% bovine serum albumin (Sigma-Aldrich, USA) for 1 hr and incubated with the primary polyclonal anti-NCX1 antibody (1:100) [16], monoclonal anti-α-smooth muscle actin (αSMA) antibody (1:100) (Dako, Denmark), or polyclonal anti-von Willebrand factor (vWF) antibody (1:50) (Proteintech, USA) for 30 min and then with the secondary antibody conjugated with Alexa Fluor 405, 488, or 594 (1:200) (Thermo Fisher Scientific, USA). Fluorescent signals were detected using a confocal laser scanning microscope FV1000 (Olympus, Japan).

*2.5. Quantification of pulmonary vascular remodeling*

Pulmonary vascular remodeling was evaluated as previously reported in a modified protocol [17]. Briefly, lung sections were immunohistochemically stained with anti-vWF and anti-αSMA antibodies. The entire slide was imaged and stitched with a Keyence BZ-9000 fluorescence microscope (Keyence, Japan).

In a blinded fashion, all vWF-positive vessels (external diameters smaller than 100 μm) on the entire slide were categorized as non-muscularized vessels (<25% αSMA staining of the medial wall area), partially muscularized vessels (25%-75% αSMA staining), and fully muscularized vessels (>75% αSMA staining) (see Fig.3D upper). All microscopic images of pulmonary vessels were quantified using the ImageJ software (NIH, USA) [18]. Fifty vessels per slide were randomly selected and analyzed. Muscularization of vessels was expressed as a percentage of each category of vessels to the total number of vWF-positive vessels.

*2.6. Real-time PCR Analysis*

Total RNA was isolated from pulmonary arteries using on RNeasy Mini kit (Qiagen, USA), and it was reverse-transcribed with a QuantiTect Reverse Transcription kit (Qiagen). Quantitative real-time PCR was performed using a QuantiTect SYBR Green PCR kit, and analyzed on StepOne Real-Time PCR System (Thermo Fisher Scientific, USA) according to manufacturer's protocol. Primers targeting the genes of interest and the housekeeping gene, namely β-actin, as an endogenous control, were used (see Supplemental Table 1).

*2.7. Statistical analysis*

Data are presented as the means ± S.E.M. Statistical comparisons were made using a one- or two-way ANOVA followed by a Student's *t*-test or Tukey's test. $P < 0.05$ was considered statistically significant. All analyses were performed using the StatFlex software (Artek, Japan).

**3. Results**

*3.1. Upregulation of NCX1 in pulmonary arteries of mice exposed to chronic hypoxia*

Prolonged exposure to normobaric hypoxia in experimental animals generates the most commonly used PAH models [5,6]. We initially examined the expression and localization of NCX1 in lung tissues of C57BL/6J mice after exposure to chronic hypoxia (10% $O_2$ for 4 weeks) by immunostaining. As shown in Fig. 1A, immunofluorescence staining of NCX1 was observed in the distal pulmonary arteries of mice. Interestingly, the immunofluorescence

intensities of NCX1 were strongly localized in the distal pulmonary arteries of hypoxic mice compared with those of normoxic mice. Consistently, hypoxic exposure significantly increased mRNA levels of NCX1, as well as vascular remodeling factors (HIF-1α, TGF-β1, and Basigin), in pulmonary arteries of C57BL/6J mice (Fig. 1B). This finding raises the possibility that upregulation of NCX1 contributes to the pathogenesis of hypoxia-induced PAH.

*3.2. Attenuation of hypoxia-induced PAH in NCX1$^{+/-}$ mice*

We used NCX1$^{+/-}$ mice, as animal models expressing half of NCX1, to examine the pathophysiological role of NCX1 in hypoxia-induced PAH. NCX1$^{+/-}$ mice were apparently normal in physiological parameters, such as systolic blood pressure, heart rate, and creatinine clearance, and organ morphology, as previously reported [10,13,15]. We confirmed that the expression of NCX1 mRNA in pulmonary arteries of NCX1$^{+/-}$ mice was approximately half of that in wild-type (WT) mice (Fig. 2A). Immunofluorescence staining also showed weak expression of NCX1 in the distal pulmonary arteries of NCX1$^{+/-}$ mice compared with those of WT mice (Fig. 2B). We compared RVSP and the weight ratio of RV/(LV+S), as an index of RV hypertrophy, between WT and NCX1$^{+/-}$ mice exposed to normoxia or chronic hypoxia (10% $O_2$ for 4 weeks). Under normoxic conditions, no significant differences were observed in RVSP and RV/(LV+S) weight ratio between WT and NCX1$^{+/-}$ mice (Fig. 2C and D). In WT mice, prolonged exposure to hypoxia induced significant elevations in RVSP and RV/(LV+S) weight ratio ($P < 0.01$). In contrast, in NCX1$^{+/-}$ mice, hypoxia-induced elevation of RVSP was partially observed, but it was significantly attenuated compared to WT mice ($P < 0.05$; Fig.

2C). Notably, $NCX1^{+/-}$ mice exposed to hypoxia did not exhibit significant increase in RV/(LV+S) weight ratio ($P > 0.05$; Fig. 2D). These results suggest that NCX1 plays a crucial role in the development of hypoxia-induced PAH.

*3.3. NCX1 inhibitor attenuates hypoxia-induced PAH in mice*

Specific NCX1 inhibitor is an effective tool for analyzing the pathophysiological roles of NCX1, and might be useful therapeutically [12]. SEA0400 is a potent and specific inhibitor of NCX1 [19]. Continuous administration of SEA0400 (0.5 mg/kg/day for 4 weeks) by osmotic pumps significantly suppressed hypoxia-induced elevation of RVSP ($P < 0.01$) in C57BL/6J mice in comparison to that in mice treated with vehicle (Fig. 3A), whereas it slightly, but not significantly, reduced hypoxia-induced elevation of RV/(LV+S) weight ratio (Fig. 3B). Moreover, we assessed the vascular density and muscularization in small pulmonary arteries of hypoxic mice treated with or without SEA0400. Interestingly, SEA0400 significantly increased non-muscularized vessels and conversely decreased partially muscularized vessels without virtually affecting fully muscularized vessels and total vessel density (Fig. 3C and D). These data suggest that NCX1 inhibitor effectively attenuates hypoxia-induced PAH in mice.

***Discussion***

PAH is a progressive and intractable disease characterized by pulmonary arterial constriction and vascular remodeling [1,2]. Prolonged exposure to hypoxia in experimental animals is commonly used as a PAH model [5,6]. Previous studies have shown that hypoxic

exposure causes abnormally enhanced $Ca^{2+}$ signaling in pulmonary artery smooth muscle cells (PASMCs), which is a major trigger for pulmonary arterial constriction and vascular remodeling [5,7], but its molecular mechanisms remain clearly unknown. Intriguingly, in PASMCs from idiopathic pulmonary arterial hypertension (IPAH) patients, NCX1 is overexpressed compared with PASMCs from normal subjects [20]. Nevertheless, the pathophysiological role of NCX1 in PAH animal models has not been critically investigated by genetic knockout and pharmacological studies. The major findings of the present study are; (i) NCX1 was upregulated in pulmonary arteries of mice exposed to chronic hypoxia (Fig. 1); (ii) in $NCX1^{+/-}$ mice, hypoxia-induced PAH and RV hypertrophy were attenuated compared to WT mice (Fig. 2); (iii) specific NCX1 inhibitor SEA0400 effectively suppressed hypoxia-induced PAH and vascular remodeling in mice (Fig. 3). Our findings provide strong evidence that the upregulation of NCX1 in pulmonary arteries contributes to the development of hypoxia-induced PAH.

NCX1 is a bidirectional $Ca^{2+}$ transporter controlled by membrane potential and transmembrane gradients of $Na^+$ and $Ca^{2+}$, which plays an important role in intracellular $Ca^{2+}$ homeostasis and $Ca^{2+}$ signaling [8,9]. Previous our studies suggest that vascular smooth muscle NCX1 normally operates in the $Ca^{2+}$ influx mode to control vascular tone and agonist-induced vasoconstriction in small resistance arteries [13,21]. Other reports indicate that NCX1 physically or functionally interacts with TRPC3 or TRPC6, a non-selective cation channel, suggesting that TRPC-mediated $Na^+$ entry may trigger the $Ca^{2+}$ influx mode of NCX1 [22,23]. Interestingly, in PASMCs (or pulmonary arteries) from IPAH patients or

hypoxia-induced PAH mice, TRPC3 and TRPC6 [24,25], as well as NCX1 [20] (Fig. 1), are upregulated. Actually, both TRPC6 and NCX1 are reported to be target genes for HIF-1α [26,27], a nuclear factor required for transcription activation in response to hypoxia. In addition, genetic knockout mice of TRPC6 and NCX1 similarly exhibit attenuation of hypoxia-induced PAH and pulmonary vascular remodeling in rodent models [25,26] (Fig. 2). Taken together, these findings suggest that enhanced $Ca^{2+}$ entry via NCX1 may contribute to pulmonary arterial constriction and vascular remodeling, leading to PAH, although further studies are necessary to elucidate the precise mechanisms.

Specific NCX1 inhibitor is an effective tool for analyzing the pathophysiological roles of NCX1, and might be useful therapeutically [12]. SEA0400 is a potent and specific NCX1 inhibitor; it only slightly inhibits NCX2 and has no effect on NCX3 [19]. Intriguingly, SEA0400 much more effectively blocks the $Ca^{2+}$ influx mode than the $Ca^{2+}$ efflux mode of NCX1 [19]. Therefore, SEA0400 preferentially protects pathologic $Ca^{2+}$ overload via the $Ca^{2+}$ influx mode of NCX1, despite having minimal effects on normal $Ca^{2+}$ metabolism via the $Ca^{2+}$ efflux mode of NCX1 [12]. Consistent with these properties, SEA0400 may effectively block enhanced $Ca^{2+}$ entry via NCX1 in pulmonary arteries, resulting in attenuation of hypoxia-induced PAH and vascular remodeling in mice (Fig. 3).

In summary, this comprehensive study using NCX1-knockout mice and specific NCX1 inhibitor reveals that the upregulation of NCX1 contributes to the pathogenesis of hypoxia-induced PAH, suggesting that NCX1 inhibition by specific inhibitors or oligonucleotide therapeutics might be a novel approach for the treatment of PAH.

**Figure Legends**

**Fig.1** Enhanced expression of NCX1 in pulmonary arteries of mice exposed to hypoxia. (A) Triple immunostaining of NCX1 (green), vWF (red), and αSMA (blue) in lung sections from C57BL/6J mice exposed to normoxia (Nor) or hypoxia (Hyp) for 4 weeks. (B) mRNA expression levels of NCX1 and vascular remodeling factors (HIF-1α, TGF-β1, and Basigin (Bsg)) in pulmonary arteries from mice under normoxic or hypoxic condition for 4 weeks. Quantitative real-time PCR was performed as described under Section 2. Data are presented as means ± S.E.M. (n=3). *$P < 0.05$, **$P < 0.01$.

**Fig.2** Attenuation of hypoxia-induced PAH in $NCX1^{+/-}$ mice. (A) Expression levels of NCX1 mRNA in pulmonary arteries from wild-type (WT) and $NCX1^{+/-}$ mice. (B) Double immunostaining of NCX1 (green) and αSMA (red) in lung sections from WT and $NCX1^{+/-}$ mice. (C) Representative traces (left) and summarized data (right) of right ventricular systolic pressure (RVSP) in WT and $NCX1^{+/-}$ mice exposed to normoxia (Nor) or hypoxia (Hypo). (D) Ratio of right ventricle weight to left ventricle and septum weights (RV/(LV+S)) in each group. Data are presented as means ± S.E.M. (n=5-7). *$P < 0.05$, **P < 0.01.

**Fig.3** NCX1 inhibitor attenuates hypoxia-induced PAH in C57BL/6J mice. (A) RVSP and (B) RV/(LV+S) weight ratio in C57BL/6J mice treated subcutaneously with SEA0400 (0.5 mg/kg/day for 4 weeks) or vehicle (50% DMSO) by Alzet osmotic pumps under hypoxic condition. (C) Total vessel densities of small pulmonary arteries (<100 μm) in lung sections from hypoxic mice treated with or without SEA0400. (D) Proportion of non-muscularized vessels (non; <25%), partially muscularized vessels (partial; 25%-75%), and fully muscularized vessels (full; >75%), as shown in examples of double staining images (upper) of small pulmonary arteries with anti-αSMA and anti-vWF antibodies. Data are presented as means ± S.E.M. (n=5). **P < 0.01.

***References***


[1] E.M.T. Lau, E. Giannoulatou, D.S. Celermajer, M. Humbert, Epidemiology and treatment of pulmonary arterial hypertension. Nat. Rev. Cardiol. 14 (2017) 603–614.

[2] A. Makino, A.L. Firth, J.X.-J. Yuan, Endothelial and smooth muscle cell ion channels in pulmonary vasoconstriction and vascular remodeling. Compr. Physiol. 1 (2011) 1555–1602.

[3] G.G. Pietra, F. Capron, S. Stewart, O. Leone, M. Humbert, I.M. Robbins, L.M. Reid, R.M. Tuder, Pathologic assessment of vasculopathies in pulmonary hypertension. J. Am. Coll. Cardiol. 43 (2004) 25S–32S.

[4] R.T. Schermuly, H.A. Ghofrani, M.R. Wilkins, F. Grimminger, Mechanisms of disease: pulmonary arterial hypertension. Nat. Rev. Cardiol. 8 (2011) 443–455.

[5] K.R. Stenmark, K.A. Fagan, M.G. Frid, Hypoxia-induced pulmonary vascular remodeling: cellular and molecular mechanisms. Circ. Res. 99 (2006) 675–691.

[6] G. Maarman, S. Lecour, G. Butrous, F. Thienemann, K. Sliwa, A comprehensive review: the evolution of animal models in pulmonary hypertension research; are we there yet? Pulm. Circ. 3 (2013) 739–756.

[7] F.K. Kuhr, K.A. Smith, M.Y. Song, I. Levitan, J.X.-J. Yuan, New mechanisms of pulmonary arterial hypertension: role of $Ca^{2+}$ signaling. Am. J. Physiol. Heart Circ. Physiol. 302 (2012) H1546–H1562.

[8] K.D. Philipson, D.A. Nicoll, Sodium-calcium exchange: a molecular perspective. Annu. Rev. Physiol. 62 (2000) 111–133.

[9] M.P. Blaustein, W.J. Lederer, Sodium/calcium exchange: its physiological implications. Physiol. Rev. 79 (1999) 763–854.

[10] N. Morimoto, S. Kita, M. Shimazawa, H. Namimatsu, K. Tsuruma, K. Hayakawa, K. Mishima, N. Egashira, T. Iyoda, I. Horie, Y. Gotoh, K. Iwasaki, M. Fujiwara, T. Matsuda, A. Baba, I. Komuro, K. Horie, J. Takeda, T. Iwamoto, H. Hara, Preferential involvement of $Na^+/Ca^{2+}$ exchanger type-1 in the brain damage caused by transient focal cerebral ischemia in mice. Biochem. Biophys. Res. Commun. 429 (2012) 186–190.

[11] T. Mera, T. Itoh, S. Kita, S. Kodama, D. Kojima, H. Nishinakamura, K. Okamoto, M. Ohkura, J. Nakai, T. Iyoda, T. Iwamoto, T. Matsuda, A. Baba, K. Omori, J. Ono, H. Watarai, M. Taniguchi, Y. Yasunami, Pretreatment of donor islets with the $Na^+/Ca^{2+}$ exchanger inhibitor improves the efficiency of islet transplantation. Am. J. Transplant. 13 (2013) 2154–2160.

[12] T. Iwamoto, Sodium-calcium exchange inhibitors: therapeutic potential in cardiovascular diseases. Future Cardiol. 1 (2005) 519–529.

[13] T. Iwamoto, S. Kita, J. Zhang, M.P. Blaustein, Y. Arai, S. Yoshida, K. Wakimoto, I. Komuro, T. Katsuragi, Salt-sensitive hypertension is triggered by $Ca^{2+}$ entry via

$Na^+/Ca^{2+}$ exchanger type-1 in vascular smooth muscle. Nat. Med. 10 (2004) 1193–1199.

[14] K. Wakimoto, K. Kobayashi, M. Kuro-O, A. Yao, T. Iwamoto, N. Yanaka, S. Kita, A. Nishida, S. Azuma, Y. Toyoda, K. Omori, H. Imahie, T. Oka, S. Kudoh, O. Kohmoto, Y. Yazaki, M. Shigekawa, Y. Imai, Y. Nabeshima, I. Komuro, Targeted disruption of $Na^+/Ca^{2+}$ exchanger gene leads to cardiomyocyte apoptosis and defects in heartbeat. J. Biol. Chem. 275 (2000) 36991–36998.

[15] Y. Gotoh, S. Kita, M. Fujii, H. Tagashira, I. Horie, Y. Arai, S. Uchida, T. Iwamoto, Genetic knockout and pharmacologic inhibition of NCX2 cause natriuresis and hypercalciuria. Biochem. Biophys. Res. Commun. 456 (2015) 670–675.

[16] T. Iwamoto,Y. Pan, T.Y. Nakamura, S. Wakabayashi, M. Shigekawa, Protein kinase C-dependent regulation of $Na^+/Ca^{2+}$ exchanger isoforms NCX1 and NCX3 does not require their direct phosphorylation. Biochemistry 37 (1998) 17230–17238.

[17] F. Dierick, T. Héry, B. Hoareau-Coudert, N. Mougenot, V. Monceau, C. Claude, M. Crisan, V. Besson, P. Dorfmüller, G. Marodon, E. Fadel, M. Humbert, E. Yaniz-Galende, J.-S. Hulot, G. Marazzi, D. Sassoon, F. Soubrier, S. Nadaud, Resident $PW1^+$ progenitor cells participate in vascular remodeling during pulmonary arterial hypertension. Circ. Res. 118 (2016) 822–833.

[18] C.A. Schneider, W.S. Rasband, K.W. Eliceiri, NIH Image to ImageJ: 25 years of image

analysis. Nat. Methods 9 (2012) 671–675.

[19] T. Iwamoto, S. Kita, A. Uehara, I. Imanaga, T. Matsuda, A. Baba, T. Katsuragi, Molecular determinants of $Na^+/Ca^{2+}$ exchange (NCX1) inhibition by SEA0400. J. Biol. Chem. 279 (2004) 7544–7553.

[20] S. Zhang, H. Dong, L.J. Rubin, J.X.-J. Yuan. Upregulation of $Na^+/Ca^{2+}$ exchanger contributes to the enhanced $Ca^{2+}$ entry in pulmonary artery smooth muscle cells from patients with idiopathic pulmonary arterial hypertension. Am. J. Physiol. Cell Physiol. 292 (2007) C2297–C2305.

[21] Y. Wang, L. Chen, M. Li, H. Cha, T. Iwamoto, J. Zhang. Conditional knockout of smooth muscle sodium calcium exchanger type-1 lowers blood pressure and attenuates Angiotensin II-salt hypertension. Physiol. Rep. 3 (2015) e12273.

[22] C. Rosker, A. Graziani, M. Lukas, P. Eder, M.X. Zhu, C. Romanin, K. Groschner, $Ca^{2+}$ signaling by TRPC3 involves $Na^+$ entry and local coupling to the $Na^+/Ca^{2+}$ exchanger. J. Biol. Chem. 279 (2004) 13696–13704.

[23] V.S. Lemos, D. Poburko, C.-H. Liao, W.C. Cole, C. van Breemen, $Na^+$ entry via TRPC6 causes $Ca^{2+}$ entry via NCX reversal in ATP stimulated smooth muscle cells. Biochem. Biophys. Res. Commun. 352 (2007) 130–134.

[24] Y. Yu, I. Fantozzi, C.V. Remillard, J.W. Landsberg, N. Kunichika, O. Platoshyn, D.D. Tigno, P.A. Thistlethwaite, L.J. Rubin, J.X.-J. Yuan, Enhanced expression of transient

receptor potential channels in idiopathic pulmonary arterial hypertension. Proc. Natl. Acad. Sci. USA 101 (2004) 13861–13866.

[25] Y. Xia, X.-R. Yang, Z. Fu, O. Paudel, J. Abramowitz, L. Birnbaumer, J.S.K. Sham, Classical transient receptor potential 1 and 6 contribute to hypoxic pulmonary hypertension through differential regulation of pulmonary vascular functions. Hypertension 63 (2014) 173–180.

[26] J. Wang, L. Weigand, W. Lu, J.T. Sylvester, G.L. Semenza, L.A. Shimoda, Hypoxia inducible factor 1 mediates hypoxia-induced TRPC expression and elevated intracellular $Ca^{2+}$ in pulmonary arterial smooth muscle cells. Circ. Res. 98 (2006) 1528–1537.

[27] V. Valsecchi, G. Pignataro, A.D. Prete, R. Sirabella, C. Matrone, F. Boscia, A. Scorziello, M.J. Sisalli, E. Esposito, N. Zambrano, G.D. Renzo, L. Annunziato, NCX1 is a novel target gene for hypoxia-inducible factor-1 in ischemic brain preconditioning. Stroke 42 (2011) 754–763.

**Acknowledgments**

We thank I. Komuro (Tokyo University) for providing NCX1$^{+/-}$ mice. This work was supported by JSPS KAKENHI Grant Numbers JP17K08610 (T.I.), JP19K07132 (S.K.), JP19K16509 (H.T.), JP19K18230 (A.N.) and a grant from Salt Science Research Foundation (No.1540).

**Appendix A. Supplementary data**

Supplementary data associated with this article can be found, in the online version, at https://.

Fig. 1 Nagata et al.

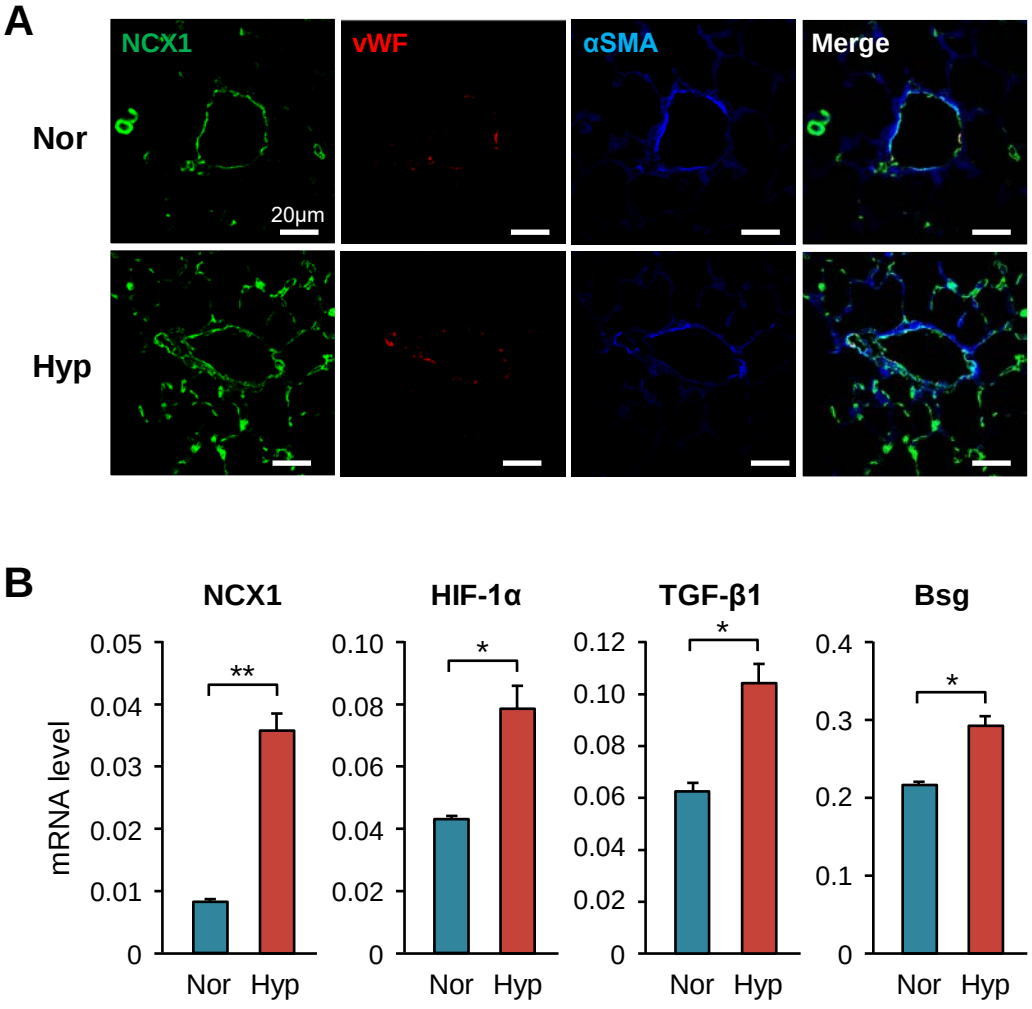

Fig. 2 Nagata et al.

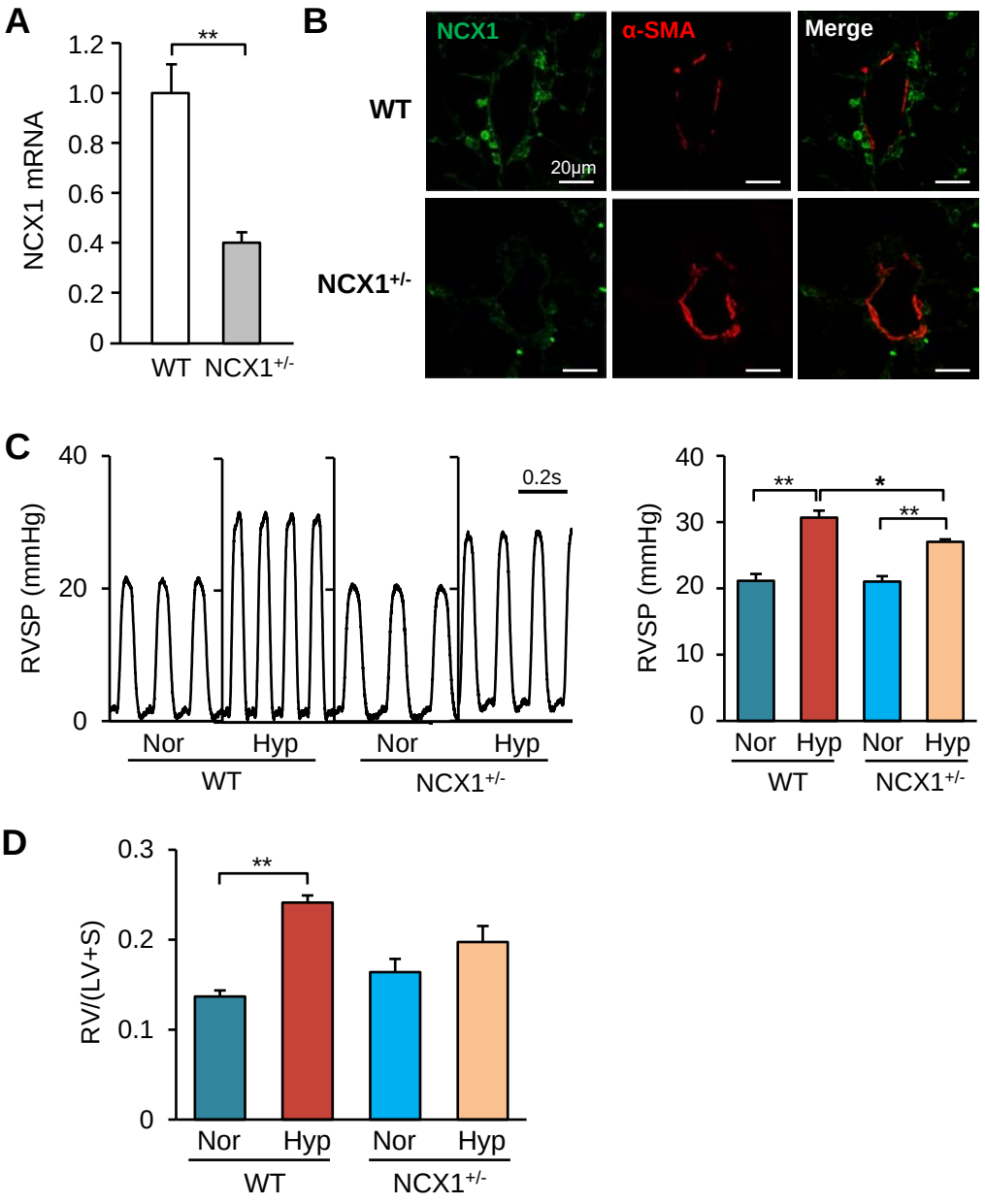

Fig. 3 Nagata et al.

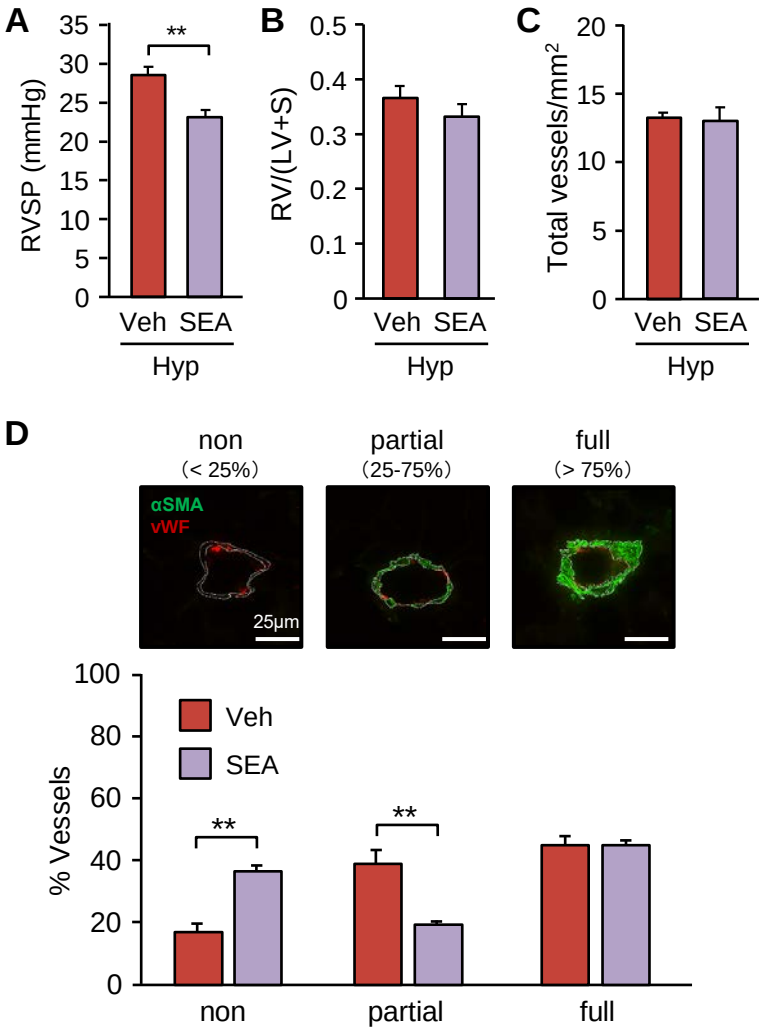

Supplemental Table 1. Primer sequences for quantitative real-time PCR

| | Forward primers | Reverse primers |
|---|---|---|
| NCX1 | 5’-TGAGAGGGACCAAGATGATG-3’ | 5’-AATGCTCGGCTTTTCTGCTG-3’ |
| HIF-1α | 5’-TGTTTGCTGAAGACACAGAG-3’ | 5’-GATCAAAGGAACGTAACTGG-3’ |
| TGF-β1 | 5’-TTGACTTTAGGAAGGACCTG-3’ | 5’-AGGACCTTGCTGTACTGTGT-3’ |
| Bsg | 5’-AATCAGAGCATTCCAGTGAG-3’ | 5’-CTATTGGTGATTGCCTCTTC-3’ |
| Actb | 5’-GGCTACAGCTTCACCACCAC-3’ | 5’-GAGTACTTGCGCTCAGGAGG-3’ |

NCX1; $Na^{+}/Ca^{2+}$ exchanger type-1, HIF-1α; hypoxia-inducible factor-1α, TGF-β1; transforming growth factor-β1, Bsg; basigin, Actb, β-actin.